electronic reprint

STRUCTURAL CHEMISTRY

ISSN: 2053-2296
journals.iucr.org/c

Isopropyl 3-deoxy-α-D-*ribo*-hexopyranoside (isopropyl 3-deoxy-α-D-glucopyranoside): evaluating trends in structural parameters

Jieye Lin, Allen G. Oliver, Reagan J. Meredith, Ian Carmichael and Anthony S. Serianni

Acta Cryst. (2021). C**77**, 490–495

STRUCTURAL CHEMISTRY
ISSN 2053-2296

Isopropyl 3-deoxy-α-D-*ribo*-hexopyranoside (isopropyl 3-deoxy-α-D-glucopyranoside): evaluating trends in structural parameters

Jieye Lin,[a] Allen G. Oliver,[a] Reagan J. Meredith,[a] Ian Carmichael[b] and Anthony S. Serianni[a]*

[a]Department of Chemistry and Biochemistry, University of Notre Dame, Notre Dame, IN 46556-5670, USA, and [b]Radiation Laboratory, University of Notre Dame, Notre Dame, IN 46556-5670, USA. *Correspondence e-mail: aseriann@nd.edu

Received 29 April 2021
Accepted 21 July 2021

Edited by I. D. Williams, Hong Kong University of Science and Technology, Hong Kong

Keywords: crystal structure; isopropyl 3-deoxy-α-D-*ribo*-hexopyranoside; isopropyl 3-deoxy-α-D-glucopyranoside; DFT; chemical synthesis.

CCDC reference: 2098123

Supporting information: this article has supporting information at journals.iucr.org/c

Isopropyl 3-deoxy-α-D-*ribo*-hexopyranoside (isopropyl 3-deoxy-α-D-glucopyranoside), $C_9H_{18}O_5$, (I), crystallizes from a methanol–ethyl acetate solvent mixture at room temperature in a $^4C_1$ chair conformation that is slightly distorted towards the $^{C5}S_{C1}$ twist-boat form. A comparison of the structural parameters in (I), methyl α-D-glucopyranoside, (II), α-D-glucopyranosyl-(1→4)-D-glucitol (maltitol), (III), and 3-deoxy-α-D-*ribo*-hexopyranose (3-deoxy-α-D-glucopyranose), (IV), shows that most endocyclic and exocyclic bond lengths, valence bond angles and torsion angles in the aldohexopyranosyl rings are more affected by anomeric configuration, aglycone structure and/or the conformation of exocyclic substituents, such as hydroxymethyl groups, than by monodeoxygenation at C3. The structural effects observed in the crystal structures of (I)–(IV) were confirmed though density functional theory (DFT) calculations in computed structures (I)[c]–(IV)[c]. Exocyclic hydroxymethyl groups adopt the *gauche–gauche* (*gg*) conformation (H5 *anti* to O6) in (I) and (III), and the *gauche–trans* (*gt*) conformation (C4 *anti* to O6) in (II) and (IV). The *O*-glycoside linkage conformations in (I) and (III) resemble those observed in disaccharides containing β-(1→4) linkages.

1. Introduction

The recent development of *MA'AT* analysis to model the conformational features of saccharides makes use of redundant NMR spin–spin coupling constants and circular statistics to obtain continuous models of molecular torsion angles in solution (Turney *et al.*, 2017; Zhang *et al.*, 2017, 2019*a*,*b*). These models can be compared to those obtained by molecular dynamics (MD) simulations to provide experimental validation of MD-derived models and an opportunity to refine force fields when needed to give MD models in better agreement with experiment. *MA'AT* analysis requires quantitative treatments of NMR spin-coupling constants to parameterize accurate equations relating them to specific molecular torsion angles in the target molecule. One of the structural factors that affects the magnitudes of *J*-couplings, especially ^1J and ^2J values, in saccharides is the conformation about exocyclic hydroxy C—O bonds appended to, or proximal to, the coupling pathways (Hadad *et al.*, 2017). Efforts have been made to investigate the conformational properties of exocyclic C—O torsion angles in saccharides (Adams & Lerner, 1992; Poppe & van Halbeek, 1994; Zhao *et al.*, 2007), but experimental characterization remains incomplete and current MD methods are unable to predict these behaviors in solution reliably. The compound discussed in this article, isopropyl 3-deoxy-α-D-*ribo*-hexopyranoside, (I) (Fig. 1), was designed to enable the

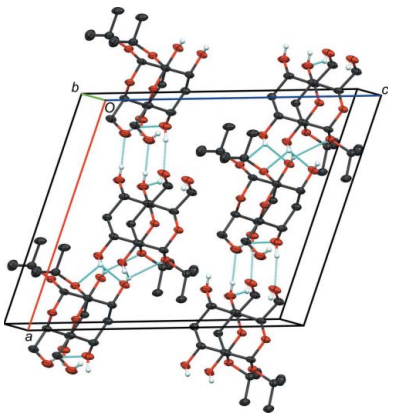

potential application of *MA'AT* analysis to investigate the conformation of the hydroxy group in solution, specifically, the conformational properties of its exocyclic C2—O2 bond. Incorporation of a relatively bulky aglycone group at C1 (isopropyl) of (I) is expected to reduce the conformational flexibility of the C1—O1 bond, which is subject to stereoelectronic constraints (Juaristi & Cuevas, 1994), while the lack of a hydroxy group at C3 eliminates contributions that C3—O3 bond rotation may make on multiple *J*-couplings sensitive to conformation of the C2—O2 bond. During ongoing NMR studies of (I), crystals were obtained and subjected to X-ray structure analysis. The results of this analysis are reported herein.

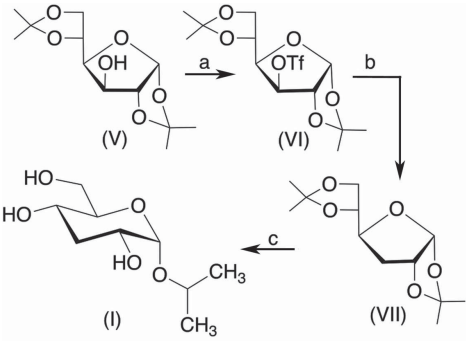

Scheme 1

2. Experimental

2.1. Synthesis and crystallization

2.1.1. Synthesis of isopropyl 3-deoxy-α-D-*ribo*-hexopyranoside, (I) (Scheme 1). Anhydrous pyridine (2.48 ml, 30.7 mmol) was added to a solution of 1,2:5,6-di-*O*-isopropylidene-α-D-glucofuranose, (V) (2.00 g, 7.7 mmol), in anhydrous CH_2Cl_2 (60 ml) at 273 K. Triflic anhydride (2.6 ml, 15.4 mmol) was added dropwise and the resulting mixture was stirred at 273 K for 2 h. The reaction was quenched by pouring the reaction mixture into ice-cold 5% aqueous $NaHCO_3$ solution (50 ml). After isolating the organic phase, the aqueous phase was extracted twice with CH_2Cl_2 (2 × 50 ml). The organic phases were combined and concentrated at 303 K *in vacuo* to give 1,2:5,6-di-*O*-isopropylidene-3-*O*-triflyl-α-D-*ribo*-hexofuranose, (VI), as a yellow solid in nearly quantitative yield (3.0 g, 7.7 mmol). NMR spectral data obtained for (VI) were consistent with those reported previously (Dias *et al.*, 2019; Russell *et al.*, 1990).

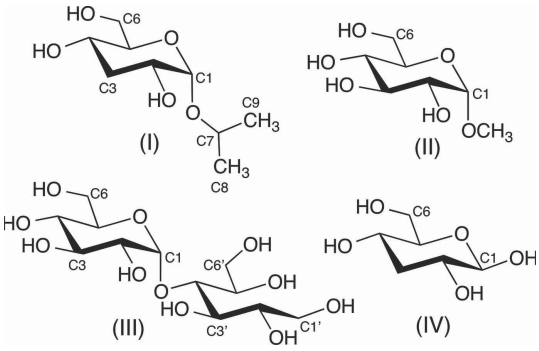

Figure 1
The chemical structures of isopropyl α-D-*ribo*-hexopyranoside, (I), methyl α-D-glucopyranoside, (II), α-D-glucopyranosyl-(1→4)-D-glucitol, (III), and 3-deoxy-β-D-*ribo*-hexopyranose, (IV). Note the unconventional numbering in (III) in which the aglycone atoms were primed to enable structural comparisons in (I)–(IV) (see text).

Table 1
Experimental details.

Crystal data	
Chemical formula	$C_9H_{18}O_5$
M_r	206.23
Crystal system, space group	Monoclinic, *I*2
Temperature (K)	120
a, *b*, *c* (Å)	13.7349 (11), 5.0575 (4), 16.0800 (12)
β (°)	109.020 (7)
V (Å^3)	1056.00 (15)
Z	4
Radiation type	Cu *Kα*
μ (mm^{-1})	0.89
Crystal size (mm)	0.34 × 0.12 × 0.07
Data collection	
Diffractometer	Bruker PHOTON-II
Absorption correction	Numerical (*SADABS*; Krause *et al.*, 2015)
T_{min}, T_{max}	0.787, 0.994
No. of measured, independent and observed [$I > 2\sigma(I)$] reflections	11702, 1976, 1889
R_{int}	0.062
(sin θ/λ)$_{max}$ (Å^{-1})	0.613
Refinement	
$R[F^2 > 2\sigma(F^2)]$, $wR(F^2)$, *S*	0.041, 0.105, 1.08
No. of reflections	1976
No. of parameters	141
No. of restraints	1
H-atom treatment	H atoms treated by a mixture of independent and constrained refinement
$\Delta\rho_{max}$, $\Delta\rho_{min}$ (e Å^{-3})	0.19, −0.24
Absolute structure	Flack *x* determined using 774 quotients $[(I^+) - (I^-)]/[(I^+) + (I^-)]$ (Parsons *et al.*, 2013)
Absolute structure parameter	0.11 (12)

Computer programs: *APEX3* (Bruker, 2018), *SAINT* (Bruker, 2018), *SHELXT2014* (Sheldrick, 2015*a*), *SHELXL2018* (Sheldrick, 2015*b*), *Mercury* (Macrae *et al.*, 2020), *XP* (Bruker, 2018), and *CIFTAB* (Sheldrick, 2008).

To a solution of (VI) (2.65 g, 6.8 mmol) in anhydrous toluene (80 ml) was added *n*-Bu_4NBH_4 (3.48 g, 13.5 mmol) and the resulting mixture was refluxed at 373 K for 4 h. The reaction was quenched by pouring the reaction mixture into ice-cold water (40 ml). The resulting mixture was extracted twice with ethyl acetate (2 × 40 ml) and the organic phases were combined and concentrated at 303 K *in vacuo* to give 1,2:5,6-di-*O*-isopropylidene-3-deoxy-α-D-*ribo*-hexofuranose, (VII), as a colorless oil in 74% yield (1.22 g, 5.0 mmol). NMR spectral data obtained for (VII) were consistent with those reported previously (Dias *et al.*, 2019).

Dowex 50 × 8 (200–400 mesh) ion-exchange resin (H^+ form) (3 g, dry weight) was added to a solution of (VII) (1.22 g, 5.0 mmol) in isopropyl alcohol (50 ml) and the resulting mixture was refluxed at 373 K for 24 h. The reaction mixture was cooled and the resin was removed by filtration.

The filtrate was concentrated at 303 K *in vacuo* to give a colorless syrup containing (I) in 90% yield. The syrup was dissolved in a minimal volume of distilled water and the solution was applied to a chromatography column (3 × 35 cm) containing Dowex 1 × 8 (200–400 mesh) ion-exchange resin in the OH^- form (Austin *et al.*, 1963). The column was eluted with distilled water at a rate of ∼1 ml min^{-1}, and fractions (∼9 ml) were collected and assayed for (I) by ^{1}H NMR. Isopropyl 3-deoxy-α-D-*ribo*-hexopyranoside, (I), eluted in fractions 22–24, which were combined and concentrated at 323 K *in vacuo* to give colorless crystals (∼0.19 g, 0.90 mmol, 18%). ^{1}H NMR (800 MHz, DMSO-d_6): δ 4.73 (*d*, *J* = 5.9 Hz, O4H, 1H), 4.63 (*d*, *J* = 3.6 Hz, H1, 1H), 4.42 (*d*, *J* = 7.2 Hz, O2H, 1H), 4.37 (*t*, *J* = 6.0, 6.6 Hz, O6H, 1H), 3.82–3.87 (*m*, CH, 1H), 3.57–3.61 (*m*, *J* = 2.3, 5.9, 11.7 Hz, H6b, 1H), 3.38–3.43 (*m*, H6a, H2, 2H), 3.29–3.32 (*m*, H5, 1H), 3.24–3.28 (*m*, H4, 1H), 1.79–1.84 (*dt*, H3b, 1H), 1.54–1.60 (*q*, H3a, 1H), 1.18 (*d*, *J* = 6.3 Hz, OCH_3, 3H), 1.09 (*d*, 6.1 Hz, OCH_3, 3H); ^{13}C NMR (200 MHz, DMSO-d_6): δ 95.7 (C1), 73.6 (C5), 68.3 (CH), 66.6 (C2), 64.6 (C4), 61.0 (C6), 36.4 (C3), 23.4 (OCH_3), 21.5 (OCH_3). HRMS (ESI–TOF) *m*/*z* [*M* + Na]$^+$: calculated for $C_9H_{18}NaO_5$ 229.1046; found 229.1061.

2.1.2. Crystallization of isopropyl 3-deoxy-α-D-*ribo*-hexopyranoside, (I). Compound (I) was dissolved in a minimal volume of a 1:1 (*v*/*v*) mixture of anhydrous methanol and ethyl acetate. The resulting solution was left at room temperature to allow the solvent to evaporate slowly. Colorless tablet-like crystals of (I) formed over a period of approximately 2 weeks.

2.2. Refinement

Crystal data, data collection and structure refinement details are summarized in Table 1. H atoms were treated with a mixture of refined and geometrically calculated atom positions. The three hydroxy H atoms were refined freely. All other H atoms were included in geometrically calculated positions, with C—H = 1.00 (methine), 0.99 (methylene), and 0.98 Å (methyl). C—H hydrogens were refined with displacement parameters tied to those of the atoms to which they were bonded, *i.e.* U_{iso}(H) = 1.2U_{eq}(C) for methine and methylene C atoms, and 1.5U_{eq}(C,O) for methyl C and hydroxy O atoms. The absolute configuration was determined by comparison with the known chirality about the molecule and by comparison of Friedel pairs of reflections (Table 1).

2.3. Density functional theory (DFT) calculations on (I)^c–(IV)^c

DFT calculations were conducted within *GAUSSIAN16* (Frisch *et al.*, 2016) using the B3LYP functional (Becke, 1993) and the 6-311+G(d,p) basis set (McLean & Chandler, 1980; Krishnan *et al.*, 1980) for geometric optimization of the structures of (I)^c–(IV)^c [the superscript 'c' distinguishes calculated structures from experimental compounds (I)–(IV)]. The only torsion-angle constraint applied during geometry optimizations of (I)^c–(IV)^c was for the C4—C5—C6—O6 torsion angle, which was fixed at 60 (*gg*), 180 (*gt*), and 300° (*tg*) to sample the three idealized exocyclic hydroxymethyl-group rotamers in each structure. All the remaining torsion angles in (I)^c–(IV)^c were optimized. All calculations included the effects of solvent water molecules, which were treated using the Self-Consistent Reaction Field (SCRF) (Cancès *et al.*, 1997) and the Integral Equation Formalism (polarizable continuum) model (IEFPCM) (Cammi *et al.*, 2000), as implemented in *GAUSSIAN16*. Bond lengths, angles, and torsion angles were extracted from optimized structures using *Python* (Jones *et al.*, 2014).

3. Results and discussion

Isopropyl 3-deoxy-α-D-*ribo*-hexopyranoside (isopropyl 3-deoxy-α-D-glucopyranoside), (I), was prepared from 1,2:5,6-di-*O*-isopropylidene-α-D-glucofuranose (Dias *et al.*, 2019) and crystallized from a mixture of methanol and ethyl acetate at room temperature to give colorless tablet-like crystals devoid of solvent (Fig. 2). Cremer–Pople puckering parameters (Cremer & Pople, 1975) for (I) and for the structurally related methyl α-D-glucopyranoside, (II) (Jeffrey *et al.*, 1977), α-D-glucopyranosyl-(1→4)-D-glucitol (maltitol), (III) (Schouten *et al.*, 1999), and 3-deoxy-α-D-*ribo*-hexopyranose, (IV) (Zhang *et al.*, 2007) (Table 2), indicate that all four structures adopt distorted $^4C_1$ chair conformations (q_3 >> q_2). The degree of distortion varies, with (III) the most distorted (q = 11°) and (II) the least distorted (q = 2°). The direction of distortion, encoded in the value of ϕ, differs in (I)–(IV), exhibiting a twist-boat distortion ($^{C5}S_{C1}$) in (I) and boat-like distortions in (II) ($^{C2,C5}B$), (III) ($B_{C2,C5}$), and (IV) ($B_{C1,C4}$).

Selected structural parameters in (I)–(IV) are listed in Table 3. Structural comparisons can be made between (I) and (II) since their aldohexopyranosyl rings are distorted in a similar manner (with similar q values), with skewing towards similar, although not identical, nonchair forms [$^{C5}S_{C1}$ in (I) and $^{C2,C5}B$ in (II)]. The hydrogen bonding in the crystals of (I) and (II) is also similar, although not identical, with atoms O2, O4, and O6 in (I), and atoms O2 and O3 in (II) serving as

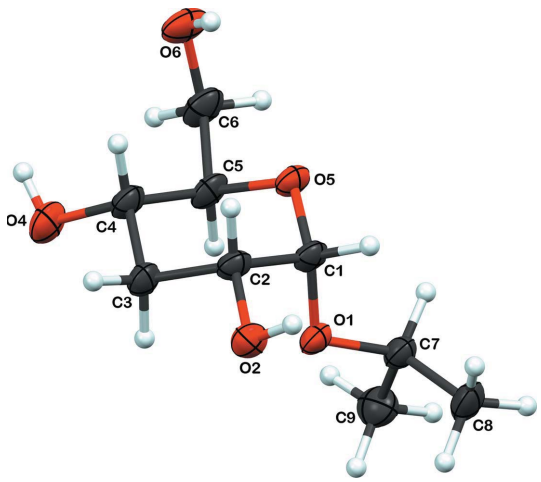

Figure 2
The molecular structure of (I), showing the atom numbering. Displacement ellipsoids are drawn at the 50% probability level and H atoms are shown as small spheres of arbitrary radii.

Table 2
Cremer–Pople structural parameters for compounds (I)–(IV).

Compound	ϕ (°)	θ (°)	Q (Å)	q_2	q_3
(I)	81 (4)	4.1 (3)	0.573 (3)	0.037 (3)	0.572 (3)
(II)	117 (6)	1.7 (2)	0.569 (2)	0.022 (2)	0.569 (2)
(III)	313.7 (8)	11.05 (15)	0.5674 (15)	0.1087 (15)	0.5569 (15)
(IV)	59.0 (16)	4.80 (14)	0.5734 (14)	0.0484 (14)	0.5714 (14)

donors and monoacceptors [O4 serves as a donor but not an acceptor, and O6 serves as a donor and dual acceptor in (II)]. While the hydrogen-bonding properties are similar, they are not likely to be equivalent in terms of the strengths of the individual interactions and their consequent effects on structural parameters. The conformation of the exocyclic hydroxymethyl group is *gg* in (I) and *gt* in (II), a significant structural difference that may affect the structural parameters (*gg* is the *gauche–gauche* conformer and *gt* is the *gauche–trans* conformer). Compound (III) differs from (I) and (II) in terms of the hydrogen bonding in that O5 serves as a monoacceptor and O6 only serves as a donor. Compound (III) adopts a *gg* conformation of the exocyclic hydroxymethyl group like (I) but unlike (II).

The exocyclic C—O bond conformations in (I)–(III) differ. The C1—C2—O2—H torsion angle is ∼72° in (I) and ∼−75° in (II). Differences such as these for C2—O2 and other C—O bonds are likely to affect structural parameters due to different interactions between oxygen lone-pair orbitals and covalent bonds in these structures (Hadad *et al.*, 2017). It is not possible at present to predict the contributions that each of these factors makes to the structural parameters, so only relatively large differences in the corresponding bond lengths, angles, and torsion angles in (I)–(III) can be interpreted with some degree of confidence.

With the above considerations in mind, the corresponding C—C bond lengths in (I)–(III) are very similar, except for the C1—C2 bond lengths. The latter differences may be caused by different C2—O2 bond conformations (Carmichael *et al.*, 1993; Hadad *et al.*, 2017; see below), slightly different values of the *phi* (ϕ) *O*-glycosidic torsion angles (see below), and/or differences in the aglycone structure. The exocyclic C—O bond lengths are very similar in (I)–(III) with two exceptions. The O1—C7 and analogous O1—C4′ bond lengths are longer in (I) and (III) than in (II), possibly due to the different aglycone size (larger aglycones correlate with longer bonds). This interpretation is supported by DFT-calculated O1—C7 and O1—C4′ bond lengths in (I)[c]–(III)[c] (Table 4). The endocyclic C—O bonds involving O5 (C1—O5 and C5—O5) are shorter in (II) than in (I) and (III), but DFT calculations indicate little difference in the C5—O5 bond lengths in (I)[c]–(III)[c], while the calculated C1—O5 bond lengths are slightly shorter in (III)[c] than in (I)[c] and (II)[c] (Table 4). These disparities may be caused by multiple structural factors, including differences in the hydrogen-bonding networks, ring distortion, and/or C1—O1 bond torsions.

The representative bond angles shown in Table 3 (C5—O5—C1, O5—C1—O1, C2—C1—O1, and C2—C2—C3) do not differ significantly in (I)–(III). This observation includes the C2—C3—C4 bond angle in 3-deoxy compound (I) and the corresponding 3-oxy compounds (II) and (III), suggesting that the loss of an equatorial O3 atom does not significantly affect the endocyclic C—C—C bond angles in the aldohexopyranosyl rings when the central C atom is the site of deoxygenation (experimental C2—C3—C4 bond angles range from 109.2 to 111.8°). The calculated C2—C3—C4 bond angles in (I)[c]–(III)[c] behave similarly, ranging from 109.7 to 110.9° (Table 4). Similar observations have been reported previously in (IV) and methyl β-D-glucopyranoside (Zhang *et al.*, 2007; Turney *et al.*, 2019). The larger C1—O1—C4′ bond angle in (III) compared to the corresponding C1—O1—C7 angles in (I) and (III) appears to stem partly from the greater steric requirements of the glucitol aglycone in (III). This angle increases with increasing

Table 3
Selected structural parameters (Å, °) in compounds (I)–(IV).

Structure parameter	Compound			
	(I)	(II)[d]	(III)[a]	(IV)
Bond lengths				
C1—C2	1.521 (3)	1.529	1.537 (2)	1.525 (2)
C2—C3	1.521 (3)	1.521	1.527 (2)	1.522 (2)
C3—C4	1.524 (3)	1.531	1.529 (2)	1.530 (2)
C4—C5	1.521 (3)	1.529	1.525 (2)	1.533 (2)
C5—C6	1.518 (3)	1.516	1.516 (2)	1.509 (2)
C1—O1	1.403 (3)	1.401	1.405 (2)	1.400 (2)
C1—O5	1.428 (3)	1.414	1.427 (2)	1.415 (2)
C2—O2	1.427 (3)	1.410	1.428 (2)	1.423 (2)
C3—O3		1.420	1.429 (2)	
C4—O4	1.434 (3)	1.414	1.426 (2)	1.432 (2)
C5—O5	1.440 (3)	1.428	1.453 (2)	1.438 (2)
C6—O6	1.415 (4)	1.421	1.419 (2)	1.429 (2)
O1—C7	1.444 (3)	1.422		
O1—C4′			1.448 (2)	
Angles				
C5—O5—C1	113.08 (19)	113.49	112.6 (1)	112.78 (10)
O5—C1—O1	112.01 (19)	113.03	111.4 (1)	105.67 (10)
C2—C1—O1	107.6 (2)	106.99	107.5 (1)	110.32 (10)
C2—C3—C4	109.7 (2)	109.24	111.8 (1)	110.76 (11)
C1—O1—C7	114.6 (2)	113.82		
C1—O1—C4′			116.2 (1)	
Torsion angles				
C1—C2—C3—C4	−55.8 (3)	−55.32	−45.6 (2)	−54.39 (14)
C1—O5—C5—C4	58.9 (3)	58.43	66.7 (1)	60.09 (13)
C4—C5—C6—O6	51.4 (3) (*gg*)	−164.33 (*gt*)	54.3 (2) (*gg*)	−165.04 (10) (*gt*)
O5—C5—C6—O6	−70.4 (3)	73.94	−64.8 (1)	74.22 (13)
C2—C1—O1—C7/C4′ (ϕ)[b]	−162.34 (18)	−175.22	−165.3 (1)	
O5—C1—O1—C7/C4′ (ϕ')	77.4 (2)	62.67	73.2 (1)	
C1—O1—C7—C8 (ψ)[c]	89.9 (2)			
C1—O1—C7—C9 (ψ')	−147.9 (2)			
C1—O1—C4′—C3′ (ψ)			94.0 (1)	
C1—O1—C4′—C5′ (ψ')			−139.1 (1)	

Notes: (*a*) In compound (III), the atoms in the aldohexopyranosyl ring are unprimed and those in the acyclic alditol aglycone are primed (see Fig. 1) to simplify structural comparisons between (I)–(IV). (*b*) Either torsion angle ϕ or ϕ' can be used to define rotation about the C1—O1 bonds in (I)–(III). (*c*) Either ψ or ψ' can be used to define rotation about the O1—C7 or O1—C4′ bonds in (I) and (III), respectively. (*d*) S.u. values were not reported in the original article. Definitions of the *gg* (*gauche–gauche*), *gt* (*gauche–trans*), and *tg* (*trans–gauche*) staggered conformers for the exocyclic hydroxymethyl groups in (I)–(IV) are as follows: *gg*, H5 *anti* to O6; *gt*, C4 *anti* to O6; *tg*, O5 *anti* to O6.

aglycone size and complexity (*i.e.* $\angle_{methyl} < \angle_{isopropyl} < \angle_{glucitol}$) within the limited set of compounds examined. This trend is similar to that found in DFT calculations for (I)^c–(III)^c, with $\angle_{methyl}$ (~114°) considerably smaller than $\angle_{isopropyl}$ (~117°) and $\angle_{glucitol}$ (~118°) (Table 3).

The experimental O5—C1—O1 and C2—C1—O1 bond angles in (IV) differ from the corresponding angles in (I)–(III), the former are considerably smaller and the latter are considerably larger. Differences in the anomeric configuration contribute to this behaviour; greater double-bond character of the O5—C1 bond in the α-anomers due to a strong *endo*-anomeric effect (Juaristi & Cuevas, 1994) leads to a larger O5—C1—O1 bond angle and possibly to a smaller C2—C1—O1 bond angle. DFT calculations are in good agreement with the experimental observations for the O5—C1—O1 bond angle, with an average value of 108° in (IV)^c and 113° in (I)^c–(III)^c (Table 4) compared to experimental values of 106 and ~112°, respectively. On the other hand, the calculated C2—C1—O1 bond angles are not much different in the four structures (Table 4).

An inspection of the C1—C2—C3—C4 and C1—O5—C5—C4 endocyclic torsion angles in (I)–(III) shows that the corresponding values in (I) and (II) are very similar, but these values differ significantly from the corresponding values in (III). This behavior is a manifestation of the slightly different ring distortions in (I)–(III), the former two only slightly distorted towards forms near $^{C5}S_{C1}$, but the latter more distorted towards the much different $B_{C2,C5}$ form. In addition, the more sterically demanding aglycone groups reduce the experimental C2—C1—O1—C7/C4′ torsion angle (values become less negative) and increase the O5—C1—O1—C7/C4′ torsion angle (values become more positive). The *exo*-anomeric effect (Juaristi & Cuevas, 1994) largely controls these *phi* (ϕ) torsion angles in which the aglycone C4′ or C7 atom is roughly *anti* to C2 in all cases. The DFT results agree qualitatively with the experimental observations, with the average calculated O5—C1—O1—C7 angle in (II)^c (71°) smaller than the corresponding average angles in (I)^c (86°) and (III)^c (97°), and the average calculated C2—C1—O1—C7/C4′ angles in (II)^c, (I)^c, and (III)^c being 192 (−168), 208 (−152), and 219° (−141°), respectively (Table 4).

The torsion angles that define *psi* (ψ) in (I) (C1—O1—C7—C8/C9) and (III) (C1—O1—C4′—C3′/C5′) are very similar (<10° differences), and mimic those found in disaccharides containing β-(1→4) *O*-glycosidic linkages. For example, the related C1—O1—C4′—C3′ and C1—O1—C4′—C5′ torsion angles in the crystal structure of methyl β-lactoside are 78.4 (2) and −161.3 (2)°, respectively (Stenutz *et al.*, 1999), comparable to values of 89.9 (2) and −147.9 (2)°, respectively, in (I). The steric factors that largely control ψ appear to be similar when the aglycone is an isopropyl group, an acyclic

Table 4
DFT-calculated bond lengths (°), angles (°), and torsion angles (°) in (I)^c–(IV)^c.

Structure	*gg*[a]	*gt*	*tg*	*gg*	*gt*	*tg*
	O1—O7 bond length			O1—C4′ bond length		
(I)^c	1.452	1.452	1.453			
(II)^c	1.431	1.431	1.431			
(III)^c				1.445	1.435	1.446
	C1—O5 bond length			C5—O5 bond length		
(I)^c	1.420	1.419	1.422	1.439	1.441	1.437
(II)^c	1.422	1.423	1.425	1.439	1.441	1.437
(III)^c	1.414	1.412	1.417	1.440	1.442	1.438
(IV)^c	1.427	1.427	1.430	1.432	1.434	1.431
	C5—O5—C1 angle					
(I)^c	115.2	115.7	115.6			
(II)^c	114.5	114.9	114.8			
(III)^c	116.0	115.8	116.0			
(IV)^c	113.8	114.1	114.3			
	O5—C1—O1 angle					
(I)^c	113.7	113.5	113.7			
(II)^c	112.5	112.7	112.5			
(III)^c	112.6	112.9	112.5			
(IV)^c	107.6	107.6	107.5			
	C2—C1—O1 angle					
(I)^c	107.1	107.5	107.3			
(II)^c	109.4	109.4	109.4			
(III)^c	109.7	107.7	109.9			
(IV)^c	109.4	109.5	109.5			
	C2–C3–C4 bond angle					
(I)^c	110.9	111.2	111.1			
(II)^c	110.4	110.6	110.5			
(III)^c	109.7	110.4	109.9			
	C1—O1—C7 angle			C1–O1–C4′ angle		
(I)^c	117.4	117.2	117.4			
(II)^c	114.1	114.1	114.2			
(III)^c				118.2	117.6	118.8
	O5—C1—O1—C7 torsion angle			O5—C1—O1—C4′ torsion angle		
(I)^c	83.0	92.7	82.2			
(II)^c	70.6	70.9	70.9			
(III)^c				101.1	86.7	103.2
	C2—C1—O1—C7 torsion angle			C2—C1—O1—C4′ torsion angle		
(I)^c	205.5	215.0	204.5			
(II)^c	192.3	192.6	192.4			
(III)^c				223.1	208.3	224.9

Note: (*a*) *gg*, *gt*, and *tg* refer to the conformation of the exocyclic hydroxymethyl group in the geometry-optimized structures (I)^c–(IV)^c (see the legend in Table 3).

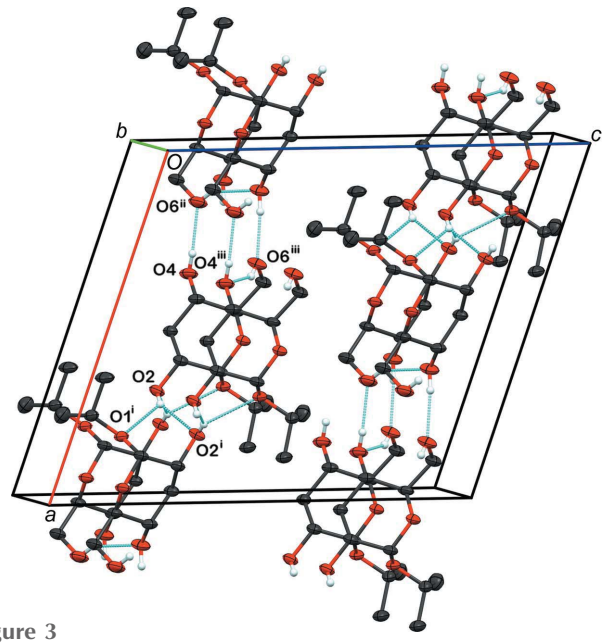

Figure 3
The packing diagram of (I), viewed along the *b* axis. Blue dashed bonds represent hydrogen-bond interactions. Atoms involved in the discussed hydrogen bonds are labelled. [Symmetry codes: (i) $-x+\frac{1}{2}, y-\frac{1}{2}, -z$; (ii) $-x+\frac{1}{2}, y+\frac{1}{2}, -z+1$; (iii) $x, y-1, z$.]

glucitol moiety, or an aldopyranosyl ring attached to O1 *via* an equatorial C—O bond.

The conformation of the exocyclic hydroxymethyl group differs in (I)–(IV), with (I) and (III) adopting the *gg* conformation (H5 *anti* to O6), and (II) and (IV) adopting the *gt* conformation (C4 *anti* to O6). In aqueous solution, *gg* and *gt* rotamers are more favored than the *tg* rotamer (O5 *anti* to O6) in the aldohexopyranosyl rings bearing an equatorial C4—O4 bond (Bock & Duus, 1994; Rockwell & Grindley, 1998; Thibaudeau *et al.*, 2004) (*tg* = *trans–gauche* conformer).

In the crystal structure of (I), four hydrogen bonds within the lattice form a dense two-dimensional sheet-like structure in the extended packing (Fig. 3 and Table 5). Atoms O4 and O6 are mutually involved in hydrogen bonds along the crystallographic screw axis; atom O4 forms a hydrogen bond to O6^{ii} [symmetry code: (ii) $-x+\frac{1}{2}, y+\frac{1}{2}, -z+1$] and in turn serves as a hydrogen-bond acceptor from O6 on an adjacent molecule (O6$\cdots$O4^{ii}). Both of these contacts adopt a (C_1^1) graph-set chain (Etter, 1990). This interaction forms a helical chain of molecules extending parallel to the *b* axis. These chains are hydrogen bonded to adjacent chains by the O2$\cdots$O1^{i} and O2$\cdots$O2^{i} bifurcated hydrogen bond [symmetry code: (i) $-x+\frac{1}{2}, y-\frac{1}{2}, -z$] that extends the sheet along the *c* direction (graph-set R_1^2). Formally, this interaction is also related by a screw axis.

Table 5
Hydrogen-bond geometry (Å, °).

D—H$\cdots$*A*	*D*—H	H$\cdots$*A*	*D*$\cdots$*A*	*D*—H$\cdots$*A*
O2—H2O$\cdots$O1^{i}	0.83 (5)	2.41 (4)	3.055 (2)	135 (4)
O2—H2O$\cdots$O2^{i}	0.83 (5)	2.27 (5)	3.025 (2)	152 (4)
O4—H4O$\cdots$O6^{ii}	0.83 (5)	1.91 (5)	2.714 (3)	163 (5)
O6—H6O$\cdots$O4^{iii}	0.78 (3)	2.07 (3)	2.772 (3)	150 (3)

Symmetry codes: (i) $-x+\frac{3}{2}, y-\frac{1}{2}, -z+\frac{1}{2}$; (ii) $-x+\frac{1}{2}, y+\frac{1}{2}, -z+\frac{1}{2}$; (iii) $x, y-1, z$.

Acknowledgements

This work was supported by the National Science Foundation and by Omicron Biochemicals, Inc., South Bend, IN. The Notre Dame Radiation Laboratory is supported by the Department of Energy Office of Science, Office of Basic Energy Sciences. This is document number NDRL 5315.

Funding information

Funding for this research was provided by: National Science Foundation, Chemistry of Life Processes (award Nos. CHE 1707660 and CHE 2002625 to Anthony S. Serianni); US Department of Energy, Office of Basic Energy Sciences (award No. DE-FC02-04ER15533 to Ian Carmichael).

References

Adams, B. & Lerner, L. (1992). *J. Am. Chem. Soc.* **114**, 4827–4829.
Austin, P. W., Hardy, F. E., Buchanan, J. G. & Baddiley, J. (1963). *J. Chem. Soc.* pp. 5350–5353.
Becke, A. D. (1993). *J. Chem. Phys.* **98**, 5648–5652.
Bock, K. & Duus, J. O. (1994). *J. Carbohydr. Chem.* **13**, 513–543.
Bruker (2018). *APEX3* and *SAINT*. Bruker AXS Inc., Madison, Wisconsin, USA.
Cammi, R., Mennucci, B. & Tomasi, J. (2000). *J. Phys. Chem. A*, **104**, 5631–5637.
Cancès, E., Mennucci, B. & Tomasi, J. (1997). *J. Chem. Phys.* **107**, 3032–3041.
Carmichael, I., Chipman, D. M., Podlasek, C. A. & Serianni, A. S. (1993). *J. Am. Chem. Soc.* **115**, 10863–10870.
Cremer, D. & Pople, J. A. (1975). *J. Am. Chem. Soc.* **97**, 1354–1358.
Dias, C., Martins, A., Pelerito, A., Oliveira, M. C., Contino, M., Colabufo, N. A. & Rauter, A. P. (2019). *Eur. J. Org. Chem.* **2019**, 2224–2233.
Etter, M. C. (1990). *Acc. Chem. Res.* **23**, 120–126.
Frisch, M. J., *et al.* (2016). *GAUSSIAN16*. Revision B.01. Gaussian Inc., Wallingford, CT, USA. https://gaussian.com/gaussian16/.
Hadad, M. J., Zhang, W., Turney, T., Sernau, L., Wang, X., Woods, R. J., Incandela, A., Surjancev, I., Wang, A., Yoon, M.-K., Coscia, A., Euell, C., Meredith, R., Carmichael, I. & Serianni, A. S. (2017). *New Developments in NMR 10: NMR in Glycoscience and Glycotechnology*, edited by T. Peters & K. Kato, pp. 20–100. London: Royal Society of Chemistry.
Jeffrey, G. A., McMullan, R. K. & Takagi, S. (1977). *Acta Cryst.* B**33**, 728–737.
Jones, E., Oliphant, T. & Peterson, P. (2014). *SciPy: Open Source Scientific Tools for Python*. https://www.scipy.org/.
Juaristi, E. & Cuevas, G. (1994). In *The Anomeric Effect*. CRC Press.
Krause, L., Herbst-Irmer, R., Sheldrick, G. M. & Stalke, D. (2015). *J. Appl. Cryst.* **48**, 3–10.
Krishnan, R. B. J. S., Binkley, J. S., Seeger, R. & Pople, J. A. (1980). *J. Chem. Phys.* **72**, 650–654.
Macrae, C. F., Sovago, I., Cottrell, S. J., Galek, P. T. A., McCabe, P., Pidcock, E., Platings, M., Shields, G. P., Stevens, J. S., Towler, M. & Wood, P. A. (2020). *J. Appl. Cryst.* **53**, 226–235.
McLean, A. D. & Chandler, G. S. (1980). *J. Chem. Phys.* **72**, 5639–5648.
Parsons, S., Flack, H. D. & Wagner, T. (2013). *Acta Cryst.* B**69**, 249–259.
Poppe, L. & van Halbeek, H. (1994). *Nat. Struct. Biol.* **1**, 215–216.
Rockwell, G. D. & Grindley, T. B. (1998). *J. Am. Chem. Soc.* **120**, 10953–10963.
Russell, R. N., Weigel, T. M., Han, O. & Liu, H. (1990). *Carbohydr. Res.* **201**, 95–114.
Schouten, A., Kanters, J. A., Kroon, J., Looten, P., Duflot, P. & Mathlouthi, M. (1999). *Carbohydr. Res.* **322**, 298–302.
Sheldrick, G. M. (2008). *Acta Cryst.* A**64**, 112–122.
Sheldrick, G. M. (2015*a*). *Acta Cryst.* A**71**, 3–8.
Sheldrick, G. M. (2015*b*). *Acta Cryst.* C**71**, 3–8.
Stenutz, R., Shang, M. & Serianni, A. S. (1999). *Acta Cryst.* C**55**, 1719–1721.
Thibaudeau, C., Stenutz, R., Hertz, B., Klepach, T., Zhao, S., Wu, Q., Carmichael, I. & Serianni, A. S. (2004). *J. Am. Chem. Soc.* **126**, 15668–15685.
Turney, T., Pan, Q., Sernau, L., Carmichael, I., Zhang, W., Wang, X., Woods, R. J. & Serianni, A. S. (2017). *J. Phys. Chem. B*, **121**, 66–77.
Turney, T., Pan, Q., Zhang, W., Oliver, A. G. & Serianni, A. S. (2019). *Acta Cryst.* C**75**, 161–167.
Zhang, W., Meredith, R., Pan, Q., Wang, X., Woods, R. J., Carmichael, I. & Serianni, A. S. (2019*a*). *Biochemistry*, **58**, 546–560.
Zhang, W., Meredith, R., Yoon, M.-K., Wang, X., Woods, R. J., Carmichael, I. & Serianni, A. S. (2019*b*). *J. Org. Chem.* **84**, 1706–1724.
Zhang, W., Noll, B. C. & Serianni, A. S. (2007). *Acta Cryst.* C**63**, o578–o581.
Zhang, W., Turney, T., Meredith, R., Pan, Q., Sernau, L., Wang, X., Hu, X., Woods, R. J., Carmichael, I. & Serianni, A. S. (2017). *J. Phys. Chem. B*, **121**, 3042–3058.
Zhao, H., Pan, Q., Zhang, W., Carmichael, I. & Serianni, A. S. (2007). *J. Org. Chem.* **72**, 7071–7082.

supporting information

Acta Cryst. (2021). C**77**, 490-495 [https://doi.org/10.1107/S205322962100749X]

Isopropyl 3-deoxy-*α*-D-*ribo*-hexopyranoside (isopropyl 3-deoxy-*α*-D-glucopyranoside): evaluating trends in structural parameters

Jieye Lin, Allen G. Oliver, Reagan J. Meredith, Ian Carmichael and Anthony S. Serianni

Computing details

Data collection: *APEX3* (Bruker, 2018); cell refinement: *SAINT* (Bruker, 2018); data reduction: *SAINT* (Bruker, 2018); program(s) used to solve structure: SHELXT2014 (Sheldrick, 2015a); program(s) used to refine structure: *SHELXL2018* (Sheldrick, 2015b); molecular graphics: *Mercury* (Macrae *et al.*, 2020) and *XP* (Bruker, 2018); software used to prepare material for publication: CIFTAB (Sheldrick, 2008).

Isopropyl 3-deoxy-*α*-<it>D</it>-*ribo*-hexopyranoside

Crystal data

$C_9H_{18}O_5$
M_r = 206.23
Monoclinic, *I*2
a = 13.7349 (11) Å
b = 5.0575 (4) Å
c = 16.0800 (12) Å
β = 109.020 (7)°
V = 1056.00 (15) Å^3
Z = 4
F(000) = 448
D_x = 1.297 Mg m^{-3}
Cu *Kα* radiation, *λ* = 1.54184 Å
Cell parameters from 9799 reflections
θ = 3.7–70.5°
μ = 0.89 mm^{-1}
T = 120 K
Tablet, colorless
0.34 × 0.12 × 0.07 mm

Data collection

Bruker PHOTON-II diffractometer
Radiation source: Incoatec micro-focus
Detector resolution: 7.41 pixels mm^{-1}
combination of *ω* and *φ*–scans
Absorption correction: numerical (SADABS; Krause *et al.*, 2015)
T_{min} = 0.787, T_{max} = 0.994
11702 measured reflections
1976 independent reflections
1889 reflections with $I > 2\sigma(I)$
R_{int} = 0.062
θ_{max} = 70.8°, θ_{min} = 3.7°
h = −16→16
k = −6→6
l = −19→19

Refinement

Refinement on F^2
Least-squares matrix: full
$R[F^2 > 2\sigma(F^2)]$ = 0.041
$wR(F^2)$ = 0.105
S = 1.08
1976 reflections
141 parameters
1 restraint
Primary atom site location: dual
Secondary atom site location: difference Fourier map
Hydrogen site location: mixed
H atoms treated by a mixture of independent and constrained refinement
$w = 1/[\sigma^2(F_o^2) + (0.0607P)^2 + 0.4315P]$ where $P = (F_o^2 + 2F_c^2)/3$
$(\Delta/\sigma)_{max} < 0.001$
$\Delta\rho_{max}$ = 0.19 e Å^{-3}
$\Delta\rho_{min}$ = −0.24 e Å^{-3}

Absolute structure: Flack *x* determined using 774 quotients [(I+)-(I-)]/[(I+)+(I-)] (Parsons *et al.*, 2013)
Absolute structure parameter: 0.11 (12)

Special details

Geometry. All esds (except the esd in the dihedral angle between two l.s. planes) are estimated using the full covariance matrix. The cell esds are taken into account individually in the estimation of esds in distances, angles and torsion angles; correlations between esds in cell parameters are only used when they are defined by crystal symmetry. An approximate (isotropic) treatment of cell esds is used for estimating esds involving l.s. planes.

Fractional atomic coordinates and isotropic or equivalent isotropic displacement parameters (Å²)

	x	*y*	*z*	U_{iso}*/U_{eq}
O1	0.68915 (12)	0.5805 (4)	0.37509 (11)	0.0263 (4)
O2	0.69471 (13)	0.4545 (4)	0.20866 (12)	0.0296 (4)
H2O	0.728 (3)	0.315 (9)	0.214 (3)	0.055 (11)*
O4	0.37421 (15)	0.7884 (5)	0.22265 (14)	0.0391 (5)
H4O	0.315 (3)	0.727 (9)	0.210 (3)	0.054 (11)*
O5	0.55131 (11)	0.2881 (4)	0.35832 (11)	0.0275 (4)
O6	0.33085 (14)	0.1938 (5)	0.32116 (15)	0.0403 (5)
H6O	0.363 (2)	0.088 (7)	0.3067 (19)	0.019 (7)*
C1	0.64012 (16)	0.3488 (5)	0.33426 (16)	0.0256 (5)
H1	0.689748	0.197906	0.351073	0.031*
C2	0.60806 (17)	0.3912 (5)	0.23532 (16)	0.0257 (5)
H2	0.575131	0.225994	0.204708	0.031*
C3	0.53099 (18)	0.6171 (5)	0.20867 (16)	0.0280 (6)
H3A	0.506808	0.637171	0.143889	0.034*
H3B	0.564478	0.784371	0.235026	0.034*
C4	0.43968 (17)	0.5601 (6)	0.24003 (17)	0.0292 (6)
H4	0.400362	0.405639	0.206740	0.035*
C5	0.47615 (17)	0.4976 (6)	0.33787 (17)	0.0299 (6)
H5	0.508077	0.659714	0.371288	0.036*
C6	0.39025 (19)	0.4035 (7)	0.37074 (18)	0.0365 (7)
H6A	0.420739	0.345331	0.432608	0.044*
H6B	0.344038	0.554464	0.369861	0.044*
C7	0.75087 (17)	0.5488 (6)	0.46627 (16)	0.0285 (6)
H7	0.721028	0.404685	0.493057	0.034*
C8	0.86015 (19)	0.4748 (7)	0.47172 (19)	0.0403 (7)
H8A	0.858502	0.317248	0.435790	0.060*
H8B	0.900822	0.437631	0.533031	0.060*
H8C	0.891504	0.621728	0.449842	0.060*
C9	0.7460 (2)	0.8055 (7)	0.51170 (19)	0.0410 (7)
H9A	0.673854	0.852857	0.501534	0.062*
H9B	0.779289	0.944714	0.488209	0.062*
H9C	0.781656	0.786285	0.574997	0.062*

Atomic displacement parameters (Å²)

	U^{11}	U^{22}	U^{33}	U^{12}	U^{13}	U^{23}
O1	0.0155 (7)	0.0324 (9)	0.0283 (8)	−0.0017 (7)	0.0035 (6)	0.0009 (7)
O2	0.0203 (8)	0.0336 (10)	0.0393 (9)	0.0035 (8)	0.0157 (7)	0.0028 (8)
O4	0.0177 (9)	0.0480 (12)	0.0507 (11)	0.0075 (9)	0.0100 (8)	0.0059 (10)
O5	0.0147 (8)	0.0357 (10)	0.0322 (8)	−0.0022 (7)	0.0080 (6)	0.0025 (8)
O6	0.0195 (9)	0.0493 (13)	0.0553 (13)	−0.0061 (9)	0.0166 (9)	−0.0035 (11)
C1	0.0135 (9)	0.0303 (14)	0.0337 (12)	−0.0008 (9)	0.0087 (8)	−0.0001 (10)
C2	0.0161 (9)	0.0291 (13)	0.0328 (11)	−0.0024 (9)	0.0092 (8)	−0.0011 (10)
C3	0.0168 (10)	0.0342 (14)	0.0324 (12)	0.0015 (10)	0.0072 (9)	0.0036 (11)
C4	0.0140 (10)	0.0350 (14)	0.0370 (13)	0.0001 (10)	0.0060 (9)	−0.0005 (11)
C5	0.0131 (11)	0.0399 (16)	0.0368 (13)	0.0011 (10)	0.0085 (9)	−0.0036 (11)
C6	0.0184 (11)	0.0542 (18)	0.0386 (13)	−0.0029 (12)	0.0116 (10)	−0.0011 (13)
C7	0.0192 (11)	0.0372 (14)	0.0268 (11)	−0.0034 (10)	0.0045 (9)	0.0037 (10)
C8	0.0177 (11)	0.0564 (18)	0.0419 (14)	0.0002 (12)	0.0030 (10)	0.0128 (14)
C9	0.0430 (15)	0.0434 (16)	0.0328 (13)	−0.0072 (14)	0.0071 (11)	−0.0003 (13)

Geometric parameters (Å, º)

O1—C1	1.403 (3)	C3—H3B	0.9900
O1—C7	1.443 (3)	C4—C5	1.521 (3)
O2—C2	1.427 (3)	C4—H4	1.0000
O2—H2O	0.83 (5)	C5—C6	1.518 (3)
O4—C4	1.434 (3)	C5—H5	1.0000
O4—H4O	0.83 (5)	C6—H6A	0.9900
O5—C1	1.428 (3)	C6—H6B	0.9900
O5—C5	1.440 (3)	C7—C9	1.502 (4)
O6—C6	1.415 (4)	C7—C8	1.521 (3)
O6—H6O	0.78 (3)	C7—H7	1.0000
C1—C2	1.521 (3)	C8—H8A	0.9800
C1—H1	1.0000	C8—H8B	0.9800
C2—C3	1.521 (3)	C8—H8C	0.9800
C2—H2	1.0000	C9—H9A	0.9800
C3—C4	1.524 (3)	C9—H9B	0.9800
C3—H3A	0.9900	C9—H9C	0.9800
C1—O1—C7	114.6 (2)	O5—C5—C4	111.04 (19)
C2—O2—H2O	105 (3)	C6—C5—C4	113.21 (19)
C4—O4—H4O	104 (3)	O5—C5—H5	108.9
C1—O5—C5	113.08 (19)	C6—C5—H5	108.9
C6—O6—H6O	114 (2)	C4—C5—H5	108.9
O1—C1—O5	112.01 (19)	O6—C6—C5	114.2 (2)
O1—C1—C2	107.6 (2)	O6—C6—H6A	108.7
O5—C1—C2	109.38 (17)	C5—C6—H6A	108.7
O1—C1—H1	109.3	O6—C6—H6B	108.7
O5—C1—H1	109.3	C5—C6—H6B	108.7
C2—C1—H1	109.3	H6A—C6—H6B	107.6

O2—C2—C3	108.6 (2)	O1—C7—C9	107.1 (2)
O2—C2—C1	111.12 (18)	O1—C7—C8	109.1 (2)
C3—C2—C1	109.8 (2)	C9—C7—C8	112.6 (2)
O2—C2—H2	109.1	O1—C7—H7	109.3
C3—C2—H2	109.1	C9—C7—H7	109.3
C1—C2—H2	109.1	C8—C7—H7	109.3
C2—C3—C4	109.7 (2)	C7—C8—H8A	109.5
C2—C3—H3A	109.7	C7—C8—H8B	109.5
C4—C3—H3A	109.7	H8A—C8—H8B	109.5
C2—C3—H3B	109.7	C7—C8—H8C	109.5
C4—C3—H3B	109.7	H8A—C8—H8C	109.5
H3A—C3—H3B	108.2	H8B—C8—H8C	109.5
O4—C4—C5	110.1 (2)	C7—C9—H9A	109.5
O4—C4—C3	108.3 (2)	C7—C9—H9B	109.5
C5—C4—C3	110.65 (18)	H9A—C9—H9B	109.5
O4—C4—H4	109.3	C7—C9—H9C	109.5
C5—C4—H4	109.3	H9A—C9—H9C	109.5
C3—C4—H4	109.3	H9B—C9—H9C	109.5
O5—C5—C6	105.7 (2)		

C7—O1—C1—O5	77.4 (2)	C2—C3—C4—C5	52.9 (3)
C7—O1—C1—C2	−162.35 (18)	C1—O5—C5—C6	−177.9 (2)
C5—O5—C1—O1	57.7 (2)	C1—O5—C5—C4	58.9 (3)
C5—O5—C1—C2	−61.5 (3)	O4—C4—C5—O5	−173.36 (19)
O1—C1—C2—O2	57.6 (2)	C3—C4—C5—O5	−53.6 (3)
O5—C1—C2—O2	179.5 (2)	O4—C4—C5—C6	67.9 (3)
O1—C1—C2—C3	−62.5 (2)	C3—C4—C5—C6	−172.3 (2)
O5—C1—C2—C3	59.4 (3)	O5—C5—C6—O6	−70.4 (3)
O2—C2—C3—C4	−177.49 (19)	C4—C5—C6—O6	51.4 (3)
C1—C2—C3—C4	−55.8 (3)	C1—O1—C7—C9	−147.9 (2)
C2—C3—C4—O4	173.7 (2)	C1—O1—C7—C8	89.9 (2)

Hydrogen-bond geometry (Å, º)

D—H···*A*	*D*—H	H···*A*	*D*···*A*	*D*—H···*A*
O2—H2*O*···O1^{i}	0.83 (5)	2.41 (4)	3.055 (2)	135 (4)
O2—H2*O*···O2^{i}	0.83 (5)	2.27 (5)	3.025 (2)	152 (4)
O4—H4*O*···O6^{ii}	0.83 (5)	1.91 (5)	2.714 (3)	163 (5)
O6—H6*O*···O4^{iii}	0.78 (3)	2.07 (3)	2.772 (3)	150 (3)

Symmetry codes: (i) −*x*+3/2, *y*−1/2, −*z*+1/2; (ii) −*x*+1/2, *y*+1/2, −*z*+1/2; (iii) *x*, *y*−1, *z*.